Semiempirical and Ab Initio Studies of the Structure and Spectroscopy of the Azo Dye Direct Blue 1: Comparison with Experiment

Laurence C. Abbott,[†] Stephen N. Batchelor,[‡] John Oakes,[‡] John R. Lindsay Smith,[†] and John N. Moore*,[†]

Department of Chemistry, The University of York, Heslington, York, YO10 5DD, U.K., and Unilever Research, Port Sunlight, Quarry Road East, Bebington, Wirral, CH63 3JW, U.K.

Received: June 25, 2004; In Final Form: September 9, 2004

The structure and spectroscopy of the bis-azo dye Direct Blue 1 have been studied using semiempirical, Hartree−Fock, and density functional theory (DFT) calculations, and the results have been compared with those from experiment. The calculated dye structure comprises two essentially identical near-planar halves with a twist about the central biphenyl bond; the structures produced by the semiempirical AM1 method and the ab initio Hartree−Fock and DFT methods were found to be similar to each other. Excited-state calculations describe the transition to the lowest excited state of Direct Blue 1 as a charge transfer from the central biphenyl group onto both naphthyl rings, along with charge redistribution within the region of the hydrazone groups. Infrared and Raman spectra calculated by ab initio methods match the experimental spectra well; by contrast, IR spectra were modeled poorly by the semiempirical AM1 method. NMR resonances calculated with the DFT methods give good correlation with the experimental NMR resonances of Direct Blue 1 in solution. Overall, the match between the calculated and experimental properties is good for this large (88-atom) molecule, demonstrating that such calculations can assist greatly in analyzing the structure and spectroscopy of azo dyes, provided that a suitable level of theory is used.

Introduction

Azo dyes are the most widely used class of dyes;[1] they are used extensively for dyeing fabrics and as colorants in inks. There is also interest in their biochemical applications, because of their ability to bind to proteins,[3,4] and in their use for optical data storage.[5−7] There is extensive literature on azo dyes, but many of these studies have provided qualitative comparisons between dyes rather than considering their detailed structure, spectroscopy, and photochemistry.

A good knowledge of the structure of a dye is key to understanding its properties and reactivity, especially the way in which its structure is modified by different solvent and solid environments. Azo dyes are difficult to crystallize, and there are relatively few examples of crystallographic structures in the literature;[2,3,8−14] most of the reported structures are for small, simple mono-azo dyes[8−13] or for azo dyes bound to proteins,[2] amino acids,[3] or a rotaxane,[14] which may distort the structure from that of the unbound dye. The structures of dyes in solution and other environments may be studied by various spectroscopic techniques. There have been some detailed reports on the vibrational spectra and assignments of small azo dyes[15−19] and azobenzenes,[20,21] as well as some large phthalocyanine dyes,[22,23] but the vibrational spectroscopy of larger azo dyes is not well characterized. The strong electronic transitions of dyes in the visible region have been investigated in detail by some authors in terms of frontier orbitals, charge densities, and the nature of the electronic transitions,[24−27] but many reports of the electronic structure have concerned structure−color relationships.[28,29]

Modern computational methods provide the ability to study the structure and spectroscopy of complex molecules via calculations which can also assist with assigning experimental data. This approach can be particularly valuable where no experimental structures are available, and where the literature is sparse on structures of similar molecules. Semiempirical methods such as MNDO,[30] PM3,[31] and AM1[32] can yield rapid results for relatively large molecules, and they are invaluable methods which are not computationally expensive. However, the results from semiempirical methods may not provide a good match with experimental data; this can be a significant problem with azo dyes, because the parameter sets on which the methods are based are not determined from azo systems. However, it is important not to dismiss calculations at a relatively low level of theory, because they can still provide useful information to aid the interpretation of experimental results.

Ab initio methods do not suffer from the parametrization problems of semiempirical methods, but they are more computationally expensive, which may limit the size of molecule that can be studied. Density functional theory (DFT) methods have been shown to yield good comparisons with experimental data, in terms of both structure and spectroscopy,[33] and they can generally be applied to larger molecules more efficiently than traditional Hartree−Fock (HF) methods, giving superior results for a given computation time. The application of DFT methods requires a choice of functional and basis set. There are many DFT functionals, and each may be suited to a specific type of calculation.[33] The basis set used for calculating molecular properties can also have a marked effect on how well the calculated properties match experimental properties. Larger basis sets will generally give a better match to experiment, but they will also require more computational power for a given

[†] The University of York
[‡] Unilever Research

10.1021/jp047234f CCC: $27.50
Published on Web 10/26/2004

CHART 1

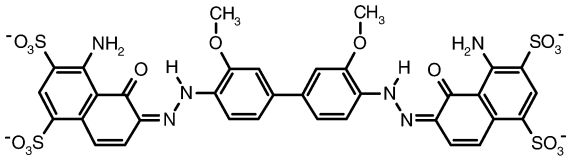

Direct Blue 1

molecule, so are not readily applicable to molecules with a large number of atoms; in these cases, calculations with a smaller basis set may give useful results.

We recently reported spectroscopic studies of the bis-azo dye Direct Blue 1 in solution and on surfaces,[34−36] in which we demonstrated that it is present as the bis-hydrazone tautomer and may undergo intramolecular hydrogen bonding. In this paper, we report the application of computational methods to explore the structure and spectroscopy of this large dye. Optimized geometries have been calculated using several semiempirical, HF, and DFT methods, and these are compared critically with crystallographic data on related dyes from the literature. Calculated molecular properties are compared with experimental UV−visible, IR, Raman, resonance Raman, and ^{1}H and ^{13}C NMR spectra, enabling a critical assessment of which calculation methods and basis sets can yield useful information on a large azo dye such as Direct Blue 1.

Experimental Section

Materials and Experimental Methods. Direct Blue 1 (Aldrich) was purified;[37] oven-dried KBr (Aldrich, FTIR grade), dimethyl sulfoxide (DMSO, Aldrich), and freshly deionized water were used without further purification. IR spectra were recorded with a Nicolet Impact 410 FTIR spectrometer, using a demountable cell (Harrick DLC-M25) with a measured path length of 56 μm and a concentration of 1×10^{-2} mol dm^{-3} for solution samples. Raman scattering was excited using either the 676.4, 647.1, 530.9, or 350.6 nm line from a Kr^{+} laser (Coherent Innova-90) or the 514.5 nm line from an Ar^{+} laser (Spectra-Physics 2025). Scattered light was collected at 90° to the incident beam, dispersed using a Spex 1403 double monochromator, and detected using a liquid-nitrogen-cooled CCD detector (Wright Instruments, Ltd.) at ca. 5-cm^{-1} resolution and an accuracy of ca. ± 2 or ± 4 cm^{-1} for visible and UV excitation, respectively. Solution samples (2×10^{-4} mol dm^{-3}) were held in a spinning quartz cell; solid KBr samples were held in a spinner and excited with the spinning surface at ca. 60° to the collection optics; laser powers were typically 30 mW for solution samples and <5 mW for KBr samples; total collection times were typically 15 min. The sample integrity following Raman data collection was checked by UV−visible spectroscopy for solution samples and visually, with a microscope, for solid samples; Raman spectra recorded at the beginning and end of the total collection time were also compared. Raman spectra were calibrated against solvent band positions and were baseline-corrected using Grams/386 (Galactic Industries Corp.).

Computational Methods. All semiempirical and ab initio calculations were performed using the *Gaussian 98* package[38] on an Intel Pentium III-based PC running Linux. Starting geometries were optimized initially using the Dreiding molecular mechanics method[39] before applying a higher-level optimization method: the MNDO,[30] PM3,[31] and AM1[32] semiempirical methods, DFT methods using the B3LYP functional,[40] and the Hartree−Fock (HF) self-consistent field method. No symmetry constraints were applied during any calculations. Standard STO-3G, 3-21G, and 6-31G(d) basis sets were used with the ab initio methods, as outlined in the text, along with a mixed basis set comprising the 6-31+G(d) basis set for N, S, and O atoms, the 6-31G(d) basis set for C atoms, and the 3-21G basis set for H atoms. The optimized structure from the B3LYP/mixed basis set calculation was used to explore the excited-state structures using both the ZINDO CIS method[41] and the time-dependent DFT (TD-DFT) method using the B3LYP functional and the 3-21G basis set; this structure was also used for NMR calculations using the GIAO method[43] with the B3LYP functional and either the mixed basis set or the 6-31G(d) basis set. Output files from calculations were parsed and analyzed using software written in-house, as well as the *Molekel* (version 4.3)[44] and *Molden* (version 4.0)[45] packages.

Results and Discussion

Geometry Optimizations. The structure of Direct Blue 1 was optimized using the MNDO, PM3, and AM1 semiempirical methods, the HF ab initio method with STO-3G and 3-21G basis sets, and the B3LYP hybrid DFT ab initio method with both the 3-21G basis set and a mixed basis set comprising the 6-31+G(d) basis set for N, S, and O atoms, 6-31G(d) for C atoms, and 3-21G for H atoms; attempts at optimization with the 6-31G(d) basis set for all atoms were unsuccessful. The mixed basis set is used in accordance with reported calculations on azobenzene, which showed that it is important to include diffuse functions on azo N atoms;[21] the smaller basis set for H atoms was required here for successful optimization at this level. In each case, the starting geometry was the hydrazone form of Direct Blue 1, as determined experimentally,[35] with the two halves of the molecule in an anti conformation around the central biphenyl bond and with the methoxy groups in a syn conformation with respect to the hydrazone NH groups.[46] Each of the sulfonate groups was protonated because test calculations on dyes with unprotonated sulfonate groups gave poor convergence and a poor match to experimental spectra; protonated sulfonate and carboxylate groups have been used for calculations on similar molecules in the literature.[15,47] The relative CPU times taken for the calculations were approximately 1:30:150:150:900 for the semiempirical−HF/STO-3G−HF/3-21G−B3LYP/3-21G−B3LYP/mixed basis set, respectively.

The optimized structure of Direct Blue 1 resulting from each method except MNDO gave two near-planar halves with a twist about the central biphenyl bond. The MNDO method gave an optimized structure which was very twisted about the hydrazone groups, forming a helix along the length of the molecule, and the naphthyl rings were severely buckled out of the plane; this structure was totally different from reported structures of azo dyes and was discounted from further study. It is likely that the MNDO parameter sets do not model hydrazone groups well. The PM3 optimized geometry was significantly more planar in each half of the molecule, with a dihedral angle of 158.1° around the bonds $N_{\sigma}-N_{\rho}-C_{11}-C_{12}$ and naphthyl rings which were slightly puckered. The AM1 and ab initio calculations all gave structures in which the main skeleton of each half was almost totally planar. The optimized structure from the highest level of theory, B3LYP/mixed basis set, would be expected to give the best optimized structure of Direct Blue 1 and is shown in Figure 1. The optimized bond lengths determined at other levels of theory show some variations from this optimized structure, but any differences are generally <5%. Selected bond lengths and angles calculated by all methods are tabulated in Table 1, with atom numbering given in Figure 2, along with experimental

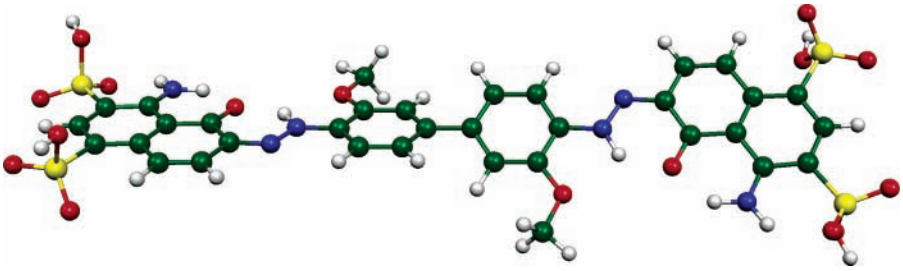

Figure 1. Optimized structure of Direct Blue 1 determined at the B3LYP/mixed basis set level.

TABLE 1: Selected Optimized Bond Lengths (Å), Angles (°), and Dihedrals (°) for Direct Blue 1 and Other Dyes from the Literature

	Direct Blue 1						other dyes (literature)		
			HF		B3LYP		X-ray diffraction		calculation
parameter	PM3	AM1	STO-3G	3-21G	3-21G	mixed[a]	hydrazone[b–f]	azo [g]	hydrazone [a,b,h]
Bond Length									
$N_\sigma-C_{10}$	1.344	1.341	1.321	1.308	1.347	1.344	1.33−1.35	1.430	1.332
$N_\sigma-N_\rho$	1.309	1.283	1.361	1.300	1.331	1.299	1.29−1.31	1.229	1.309
$N_\rho-C_{11}$	1.446	1.426	1.427	1.398	1.393	1.403	1.40−1.41	1.440	1.402
$N_\rho-H_\alpha$	1.017	1.016	1.038	1.010	1.048	1.038			1.037
C_1-C_{10}	1.443	1.453	1.467	1.433	1.429	1.431		1.400	
C_1-C_2	1.348	1.348	1.325	1.331	1.355	1.361			
C_2-C_3	1.446	1.443	1.477	1.448	1.441	1.442			
C_3-C_8	1.401	1.402	1.399	1.402	1.424	1.433			
C_9-C_{10}	1.468	1.482	1.499	1.453	1.458	1.464	1.45−1.46	1.380	1.476
C_9-O_9	1.248	1.253	1.247	1.250	1.293	1.280	1.25−1.27		1.269
$C_{14}-C_{14}'$	1.470	1.462	1.506	1.487	1.482	1.482		1.480	
$O_9\cdots H_\alpha$	1.847	2.087	1.642	1.670	1.833	1.750			1.769
$O_9\cdots H_{\beta 2}$	1.821	1.990	1.806	1.737	1.807	1.775			
$O_6\cdots H_{\beta 1}$	1.833	2.248	1.511	1.929	1.872	2.006			
Angle									
$C_{10}-N_\sigma-N_\rho$	122.7	124.9	115.9	123.2	118.4	120.0	118−119	112.2	
$N_\sigma-N_\rho-C_{11}$	119.7	121.7	120.8	120.2	120.3	120.9	119−123	114.3	
Dihedral									
$C_{13}-C_{14}-C_{14}'-C_{13}'$ [i]	48.6	41.8	38.5	50.6	40.2	35.2	39.8[f]	25.0	
$C_1-C_{10}-N_\sigma-N_\rho$	178.2	179.9	179.2	179.3	179.3	179.6	178−180		
$C_{10}-N_\sigma-N_\rho-C_{11}$	175.6	179.6	179.9	180.0	179.8	179.6	177−180	178.6	
$N_\sigma-N_\rho-C_{11}-C_{12}$	158.1	179.5	180.0	179.7	180.0	179.9	175−179	173.0	
$C_6-C_7-N_7-H_{\beta 2}$	170.8	179.4	173.4	178.4	179.4	178.1			

[a] Basis set: 6-31+G(d) for N, S, and O; 6-31G(d) for C; and 3-21G for H. [b] 1-phenylazo-2-hydroxynaphthyl dyes in the hydrazone form. [c] Reference 8. [d] Reference 9. [e] Reference 10. [f] Reference 14. [g] Reference 2. [h] Reference 56: B3LYP/mixed basis set. [i] From anti conformation.

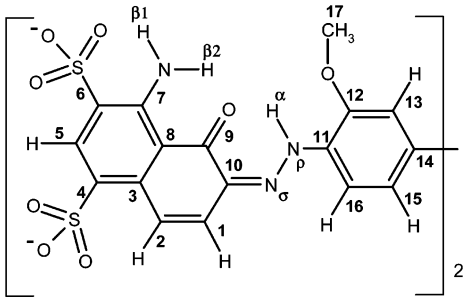

Figure 2. Atom numbering for Direct Blue 1. A number with a prime suffix denotes the equivalent atom in the other half of the molecule.

and calculated values for other dyes in the literature. For comparison, the AM1 calculation gave a geometry which was relatively close to that from the B3LYP/mixed basis calculation in almost one-thousandth of the CPU time.

The two halves of Direct Blue 1 were calculated to have nearly identical structures, with equivalent bond lengths in each half differing by ≪1%. Any asymmetry between the two halves was greater using the semiempirical methods, with the largest differences being in the bonding around the hydrazone group; the HF and DFT methods gave geometries where equivalent bond lengths in each half were identical to ≥4 significant figures, and the overall structure approached C_2 symmetry. Direct Blue 1 is a large and flexible molecule with several possible conformers, and its instantaneous structure in room temperature solution, or within a microporous solid like cellulose, is unlikely to be symmetric; our experimental studies focus on Direct Blue 1 in these environments and so we chose not to apply any symmetry constraints to our calculations.

The calculated dihedral angle about the central biphenyl group of Direct Blue 1, $C_{13}-C_{14}-C_{14}'-C_{13}'$, was found to be ca. 35−50° (measured from an anti conformation), depending on the method used. Experimental studies give a central dihedral angle of 40° for a similar bis-azo dye encapsulated in a rotaxane[14] and 25° for Congo Red bound to insulin,[16] and calculations on Congo Red, Evans Blue, and Trypan Blue give central dihedral angles of ca. 25−50°,[47] depending on the level of theory ranging from HF to molecular mechanics. Biphenyl is reported to have a central dihedral angle of 44° in the gas phase, with a low torsional barrier.[48,49] The central dihedral angles calculated here for Direct Blue 1 are comparable to those found for these similar dyes and for biphenyl both experimentally[48] and computationally;[49−51] by comparison with biphenyl, it may be expected that Direct Blue 1 also has a low barrier for rotation around the central bond. The central $C_{14}-C_{14}'$ bond length of 1.46−1.51 Å calculated for Direct Blue 1 is comparable with the reported lengths of 1.493 and 1.507 Å for the crystal structure of biphenyl.[52,53]

Each of the hydrogen atoms (H_α, $H_{\beta 1}$, and $H_{\beta 2}$) attached to the nitrogen atoms in Direct Blue 1 is calculated to be <2.6 Å

CHART 2

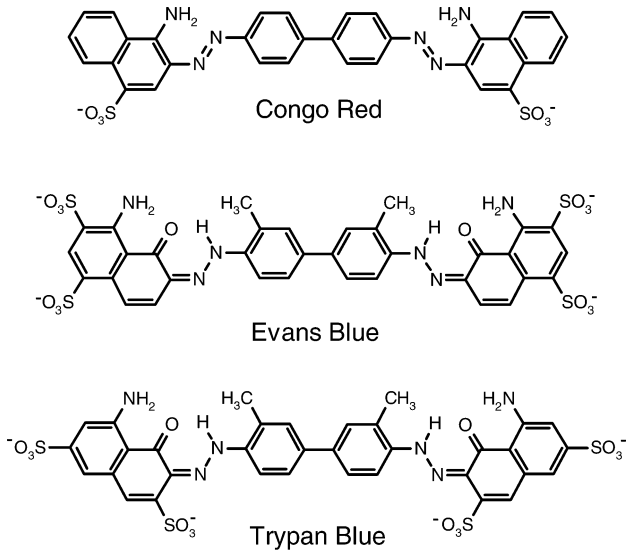

from neighboring oxygen atoms (Table 1), that is, separated by less than the sum of their van der Waals radii, indicating that intramolecular hydrogen bonding occurs in the isolated molecule. This results in a six-atom hydrogen-bonding network external to the naphthyl ring ($O_6-H_{\beta 1}-N_7-H_{\beta 2}-O_9-H_\alpha$), and this increased molecular rigidity may be expected to affect the properties of Direct Blue 1 under conditions which favor internal rather than external hydrogen bonding.[35] Significant discrepancies between the different calculated structures are revealed when the hydrogen-bonding interactions are considered; for example, the $O_9\cdots H_\alpha$ distance is calculated to be 20% longer with the AM1 method than with the B3LYP/mixed basis method (Table 1). The mixed basis set used here has diffuse functions on the oxygen and nitrogen atoms, which should give more realistic modeling of hydrogen-bonding interactions. A recent study combining crystallography and DFT calculations of simple phenylazonaphthols[54] reported hydrazone hydrogen bonds ($C=O\cdots H-N$) to be ca. 1.7 Å, both experimentally and computationally, similar to the values calculated here for $C_9=O_9\cdots H_\alpha-N_\rho$ in Direct Blue 1.

Although the literature contains relatively few reports of azo dye crystallographic structures, especially ones directly comparable with Direct Blue 1, Table 1 lists some literature values for comparison. Most of the calculated bond lengths from the B3LYP/mixed basis set calculation are within the range of those from X-ray diffraction studies of other dyes known to be predominantly in the hydrazone form; an exception is the C_9-O_9 bond of Direct Blue 1, which is calculated to be slightly longer than the crystallographic values and may arise from the extended hydrogen-bonding network. Nevertheless, the calculated C_9-O_9 bond length is reasonable, lying between the experimental C−O bond lengths in benzophenone (1.14 Å) and phenol (1.36 Å).[55]

Other bond lengths calculated at the B3LYP/mixed basis set level also may be compared with bond lengths in other molecules. The C_9-C_{10} bond length of 1.464 Å determined here is significantly longer than 1.37 Å in naphthalene;[55] and other bond lengths in this ring are longer and show more variation than the equivalent bonds in the other ring (C_3 to C_8) of the naphthyl group, reflecting the reduced aromaticity due to the hydrazone structure. Overall, the calculated bond lengths of Direct Blue 1 are also comparable with the bond lengths of Sudan III calculated using the B3LYP functional with the same mixed basis set.[56] Congo Red has a similar skeleton to Direct Blue 1, but it provides structural parameters of a purely azo form for comparison: the calculated $N_\sigma-N_\rho$ and C_9-C_{10} bonds are significantly longer, and the $N_\sigma-C_{10}$ bond is significantly shorter in the optimized geometry of Direct Blue 1 than in Congo Red,[2] showing the differences in bonding between hydrazone and azo tautomers.

CHART 3

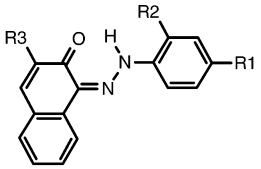

	R1	R2	R3
Solvent Yellow 14:	H	H	H
Orange II:	SO_3^-	H	H
Pigment Ca4B:	CH_3	SO_3^-	CO_2^-
Sudan III:	N=N-Ph	H	H

In summary, the optimized geometries of Direct Blue 1 calculated at a range of levels show that the DFT method with the mixed basis set gives an optimized geometry which most closely matches the crystallographic structures of similar azo dyes. Semiempirical methods give calculated structures which vary considerably between the methods tested, with the AM1 method giving a structure which most closely matches that from the DFT calculation in a small fraction of the CPU time.

Electronic Structure. The frontier orbitals, namely the HOMO−1, HOMO, LUMO, and LUMO+1 of Direct Blue 1 calculated for the optimized B3LYP/mixed basis set structure are shown in Figure 3 and discussed in the following text. Orbitals from the AM1 and HF/3-21G methods were calculated to have similar forms, with the only significant difference being

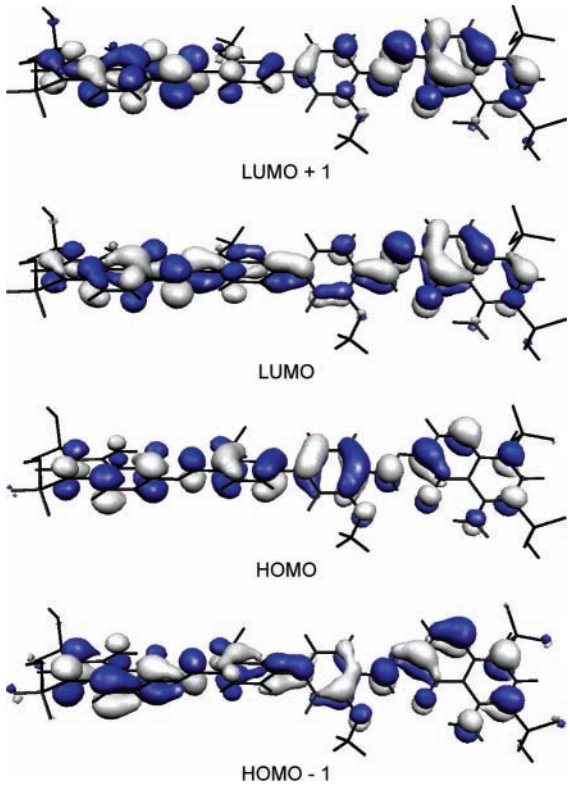

Figure 3. Representations of the HOMO−1, HOMO, LUMO, and LUMO+1 orbitals of Direct Blue 1 determined at the B3LYP/mixed basis set level.

TABLE 2: ZINDO and TD-DFT Calculated Transition Energies (*E*'s), Wavelengths (λ's), and Oscillator Strengths (*f*'s) for Singlet Excited States of Direct Blue 1

excited state[a]	ZINDO			TD-DFT B3LYP/3-21G			description
	E/eV	λ/nm	*f*	*E*/eV	λ/nm	*f*	
1	2.43	510	1.986	2.40	517	2.023	biphenyl → naphthyl, hydrazone
2	2.67	464	0.001	2.65	467	0.000	biphenyl → naphthyl, hydrazone
3				2.88	431	0.000	naphthyl, hydrazone
4				2.98	417	0.460	naphthyl, hydrazone
5	3.01	412	0.001	3.00	414	0.003	naphthyl
6	3.01	412	0.001	3.00	414	0.013	naphthyl
7	3.58	346	0.042	3.16	392	0.001	NH_2, naphthyl → hydrazone, naphthyl
8				3.17	391	0.000	NH_2, naphthyl → hydrazone, naphthyl
9				3.45	359	0.036	biphenyl → hydrazone
10	4.09	303	0.089	3.48	348	0.006	biphenyl → hydrazone

[a] Excited-state numbering from the TD-DFT calculation.

that the AM1 LUMO and LUMO+1 orbitals were slightly more polarized toward the ends of the molecule.

Each of the frontier orbitals is delocalized over the whole of the main skeleton of the dye. Both the HOMO and the LUMO+1 are antibonding across the central biphenyl bond; conversely, the HOMO−1 and the LUMO are bonding across the central biphenyl bond. Close inspection of the HOMO−1 and the HOMO shows that the main features of these two orbitals are similar, apart from equivalent regions on either side of the central bond of the molecule having the same phase for the HOMO−1 orbital and the opposite phases for the HOMO. Likewise, the LUMO and LUMO+1 show this in-phase and out-of-phase relationship, respectively, across the central region of the molecule. The two orbitals within each of these pairs are relatively close in energy, with separations of 0.36 and 0.25 eV, respectively, compared with a separation of 2.47 eV between the HOMO and LUMO.

Singlet excited-state calculations were performed on the B3LYP/mixed basis set optimized geometry using the semiempirical ZINDO method and the TD-DFT method at the B3LYP/3-21G level; attempted calculations using the TD-DFT method at the B3LYP/6-31G(d) level, or with the PBE0 functional[57] and either the 6-31G(d) or 3-21G basis set, failed to converge. Our discussion focuses on the results of the ab initio TD-DFT calculation; those from the ZINDO method were reasonably similar, as will be discussed, and took a considerably shorter CPU time (ca. 85:1). Calculated transition energies and oscillator strengths for the first ten excited states determined using the TD-DFT method are listed in Table 2, with orbital contributions listed in Table S1 (Supporting Information). The first ten excited states determined by the ZINDO method are detailed in Table S2, with those that give a change in electron density on excitation that is equivalent to one of the TD-DFT excited states being listed also in Table 2.

The lowest electronic transition calculated by the TD-DFT method is essentially a pure HOMO to LUMO transition (Table S1), with an energy of 2.40 eV (517 nm) and an oscillator strength of 2.023; that from the ZINDO calculation has a comparable energy of 2.43 eV (510 nm) and oscillator strength of 1.986, but it comprises components of HOMO to LUMO and HOMO−1 to LUMO+1 transitions (Table S2 in Supporting Information). Experimentally, Direct Blue 1 shows a very intense visible absorption band at 620 nm (2.00 eV) in water[35] with an oscillator strength of 1.286 ($\epsilon_{max} = 8 \times 10^4$ dm^3 mol^{-1} cm^{-1});[35,36] the calculated energies do not match the experimental values particularly well, but the transitions calculated by both the TD-DFT and ZINDO methods are in the visible region with very high oscillator strengths. Excited-state calculations such as those presented here are reported to give large differences of up to ca. 0.7 eV from experiment for small azo and hydrazone dyes, with flexible molecules giving poor matches.[58] Furthermore, the calculations performed here are on isolated, rather than solvated, molecules; the electronic structures of azo dyes can be affected strongly by solvent, including the preferential stabilization of one tautomer over the other, and this may account for some of the differences between the calculated and experimental transition energies.

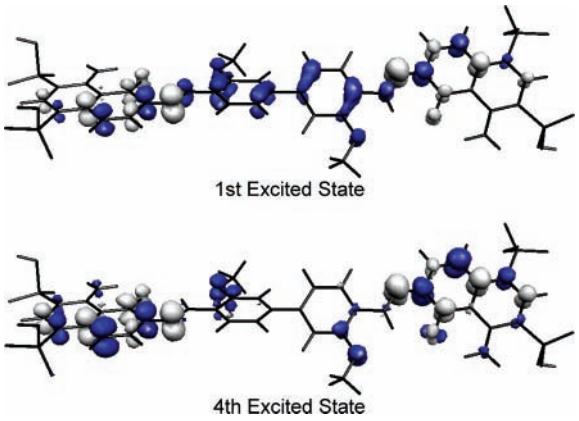

Figure 4. Calculated changes in electron density on excitation to the first and fourth singlet excited states of Direct Blue 1 determined at the B3LYP/3-21G TD-DFT level using the B3LYP/mixed basis set geometry. Blue and white regions represent a decrease and increase of electron density on excitation, respectively.

The changes induced by the excitation of Direct Blue 1 were studied by comparing the overall electron densities in the ground and excited states. Figure 4 shows plots of the calculated difference in electron density between the ground state and the first and fourth excited states from the TD-DFT calculation, with blue and white regions showing a decrease and increase in electron density on excitation, respectively. Similar figures for other excited states determined from both TD-DFT and ZINDO calculations are given in Supporting Information Figures S1 and S2, respectively, and a comparison of these figures shows the match between the excited states calculated by the TD-DFT and ZINDO methods given in Table 2.

The general form of the lowest-energy transition of Direct Blue 1 is a charge transfer from the central biphenyl moiety onto the naphthyl moieties; there is also some charge redistribution around the hydrazone groups. These changes in electron density are almost identical to those calculated using a Pariser−Parr−Pople molecular orbital (PPP-MO) method for the lowest electronic transition of a simple mono-azo dye in the hydrazone form,[28] apart from the charge redistribution being symmetrically away from the center of the molecule in the bis-azo dye Direct

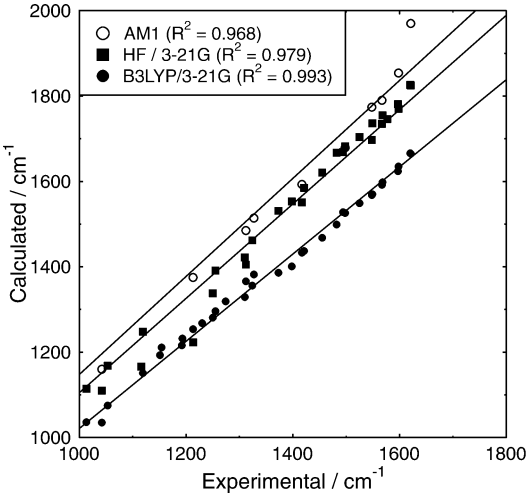

Figure 5. Linear fits of calculated to experimental wavenumbers ($y = mx$) to determine average scaling factors for AM1, HF/3-21G, and B3LYP/3-21G vibrational calculations; correlation coefficients are given in the legend.

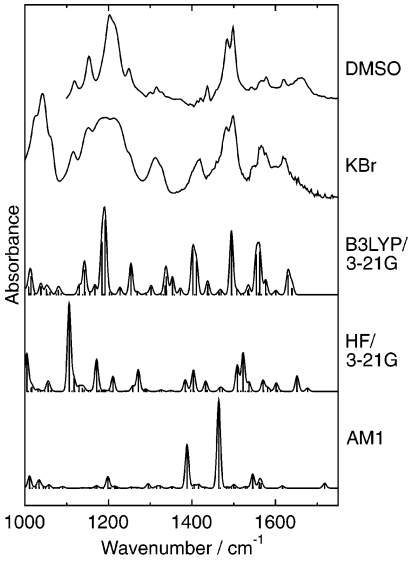

Figure 6. Experimental and calculated IR spectra of Direct Blue 1. Calculated spectra are represented both as discrete lines, scaled to the calculated intensity, and as a calculated spectrum with a fwhm Gaussian bandwidth of 10 cm^{-1} for each vibrational line.

Blue 1. The lowest four singlet excited states from the TD-DFT calculation involve some or all of the HOMO−1, HOMO, LUMO, and LUMO+1 orbitals, which are similar in form (described already), resulting in changes on excitation that involve increases and decreases in electron density on the same set of atoms (Figure S1). However, the magnitudes of the changes on these atoms differ between the four excited states; they depend on the specific orbital contributions and result in different transition energies and oscillator strengths (Table S1).

The fifth through eighth singlet excited states from the TD-DFT calculation mainly involve charge redistribution within the naphthyl rings and the hydrazone groups, and the ninth and tenth involve charge transfer from the biphenyl group mainly onto the hydrazone group (Figure S1). The fifth and sixth excited states were calculated to be near-degenerate pairs, with each transition within the pair involving charge redistribution localized at opposite ends of the molecule; these asymmetric pairs of excited states may arise from the slight asymmetry in the calculated orbitals.

Infrared and Raman Spectroscopy. Vibrational calculations were performed for Direct Blue 1 using the AM1 semiempirical method and the HF and B3LYP ab initio methods with the 3-21G basis sets; attempts with the mixed basis set were unsuccessful. All vibrational calculations were performed at the optimized geometry of the respective method, and no imaginary frequencies were found, indicating that the geometries are local minima on the potential energy surfaces. IR intensities were calculated with all three of these methods; Raman intensities were calculated with the HF and DFT methods. The protonated form of Direct Blue 1 used for the calculations contains 88 atoms resulting in 258 normal modes, which makes cross-referencing to experimental spectra challenging. To simplify the matching process, calculated spectra were created by applying a 10 cm^{-1} full bandwidth Gaussian function scaled to the relevant intensity of each of the calculated vibrational energies, and these calculated spectra were compared with the experimental spectra using both intensity and band position as a guide. A linear fit of band positions in the calculated versus experimental spectra of KBr samples (Figure 5) gave scaling factors of 0.8718, 0.9049, and 0.9791 for the AM1, HF/3-21G, and B3LYP/3-21G calculated spectra, respectively; the inclusion of a variable offset in the linear fit did not improve the fits significantly.[59] The scaling factor determined here for the AM1 calculation is slightly lower than the range of 0.9−0.9532 reported previously,[17,60] but the spread of deviations between calculated and experimental values is expected to be high for AM1,[60] as is shown in Figure 5. The scaling factor determined here for the HF/3-21G calculation compares well with that of 0.9085 reported previously,[60] and the B3LYP/3-21G scaling factor here is comparable to those reported for B3LYP with larger basis sets, such as 0.9614 for the 6-31G(d) basis set.[60] The scaling factors determined here were applied to the calculated vibrational wavenumbers; the band positions of the scaled calculated IR and Raman spectra, rather than the calculated wavenumbers of individual modes, are listed in Tables 3 and 4, respectively, along with experimental IR and Raman band positions for comparison. The use of band positions from the calculated spectra simplifies the process of matching experimental bands when there are many closely spaced calculated vibrations.

Figure 6 shows the calculated IR spectra of Direct Blue 1 along with experimental IR spectra in DMSO solution and in KBr. For a large molecule with a vibrational spectrum of this complexity, the spectrum calculated with the B3LYP method compares well with the experimental IR spectra in terms of band positions and intensities. The comparison between the experimental spectra and that calculated with the HF method is not as good as for the B3LYP method, with most of the experimental bands reproduced but with a poorer match of band intensity. The AM1 spectrum reproduces the experimental IR spectra poorly. Figure 7 shows the calculated Raman spectra of Direct Blue 1 with an experimental off-resonance Raman spectrum of Direct Blue 1 in water for comparison. Both HF and B3LYP calculated spectra match well with the experimental Raman spectrum, in terms of both band positions and intensities.

Reported DFT vibrational calculations on smaller molecules have shown that the B3LYP functional with larger basis sets such as 6-31G(d), 6-31G(d,p), and 6-31+G(d) produce calculated vibrational spectra which are superior in terms of band position and intensities[61,62] to those produced with the 3-21G basis used here for calculations on Direct Blue 1. However, the results of the HF/3-21G and B3LYP/3-21G calculations presented here show that good correlations between experimental and calculated spectra can be obtained for a large molecule with this smaller basis set. The good match between the calculated

TABLE 3: Experimental and Calculated IR Band Positions (cm^{-1}) of Direct Blue 1[a]

experiment		calculated			
KBr	DMSO	AM1	HF/3-21G	B3LYP/3-21G	description[b]
	1662 m		1677 w		$\delta(NH_\beta)$ scissor, $\delta(NH_\alpha)$, $\nu(C_9-O_9)$
1621 m	1620 w	1717 w	1651 m	1631/1640 s	$\delta(NH_\beta)$ scissor, $\delta(NH_\alpha)$, $\nu(C_9-O_9)$, δ(naph)
1598 w	1598 m	1616 w	1602 m	1601 w	ν(Ph) 8a, δ(Ph) 9a
1577 w	1577 m		1581 w	1576 m	$\delta(NH_\alpha)$, $\nu(C_9-O_9)$, $\nu(C_7-NH_2)$, δ(naph), ν(Ph) 8b, δ(Me) umbrella
1567 m	1566 m	1563 m	1570 m	1559 s	$\delta(NH_\alpha)$, $\delta(NH_\beta)$ rock, ν(Ph) 8a, δ(Ph) 3, $\nu(C_9-O_9)$, δ(naph)
1548 w	1542 w	1545 m	1536 w	1535 w	$\delta(NH_\alpha)$, $\delta(NH_\beta)$ scissor, δ(naph), δ(Ph), $\nu(C_{11}-N_\rho)$, δ(Me)
1498 vs	1498 vs	1464 vs	1523 s	1494 vs	$\delta(NH_\alpha)$, δ(naph), δ(Me) umbrella, $\nu(C_{10}-N_\sigma)$, $\nu(C_{11}-N_\rho)$, $\nu(C_7-NH_2)$, $\delta(NH_\beta)$ scissor
1482 vs	1484 vs		1509 s	1468 w	δ(Me) umbrella, δ(Ph) 18a, $\delta(NH_\alpha)$, δ(naph), $\nu(C_9-O_9)$, $\nu(C_7-NH_2)$, $\delta(NH_\beta)$ rocking
1449 sh	1437 m		1433/1469 w	1438 m	$\delta(NH_\beta)$ rocking, $\nu(C_{10}-N_\sigma)$, $\delta(NH_\alpha)$, $\nu(C_7-NH_2)$, $\nu(C_9-O_9)$, δ(Me) umbrella
1417 s	1420 w	1388 s	1384/1404 s	1403/1409 s	$\nu(C_{10}-N_\sigma)$, $\nu(C_9-O_9)$, $\delta(NH_\beta)$, δ(naph), ν(Ph) 19b, δ(Ph) 18b
1327 sh	1328 w	1320 w		1353 m	$\nu(C_{10}-N_\sigma)$, $\nu(C_{11}-N_\rho)$, δ(naph), δ(Ph) 18a, $\delta(NH_\beta)$ rocking
1312 s	1315 m	1295 w	1271 s	1338 s	δ(naph), $\delta(NH_\beta)$, $\nu(C_7-NH_2)$, $\delta(NH_\alpha)$
	1300 w			1302 m	δ(naph), ν(Ph) 14, δ(Ph) 3, $\delta(NH_\alpha)$, δ(azo), $\delta(NH_\beta)$, δ(Me) umbrella
1250 sh	1249 m		1211 m	1254 m	ν(Ph) 14, δ(Ph) 18a, $\nu(C_{12}-OMe)$, $\delta(NH_\alpha)$, $\nu(C_{11}-N_\rho)$, δ(Me) umbrella
1213 m	1215 sh		1172 s	1228 w	ν(N−N), δ(Ph) 9a, $\delta(NH_\beta)$ rocking, δ(naph), δ(Me) rocking
1192 m	1203 vs	1199 m	1106 vs	1190 vs	$\delta(NH_\alpha)$, δ(Ph) 9a, δ(Me) rocking, ν(N−N), $\delta(NH_\beta)$ rocking
1151 m	1153 sh			1143 m	$\delta(SO_3H)$, $\delta(NH_\beta)$ rocking, δ(naph)
1116 m	1119 m		1056 m		δ(naph), δ(Ph) 18b, $\delta(NH_\alpha)$
1060 s					
1042 vs		1012 m	1005 vs	1013 s	$\nu(C_{12}-OMe)$, δ(Me) umbrella, δ(Ph), δ(azo), δ(naph), $\delta(NH_\beta)$ rocking
1025 s					

[a] Calculated positions are scaled, as outlined in the text. vs = very strong; s = strong; m = medium; w = weak. [b] From B3LYP/3-21G calculation (or from HF/3-21G calculation where not possible) in decreasing degree of distortion; δ(naph) and δ(Ph) describe a general distortion of a naphthyl or phenyl moiety, respectively (numbers indicate approximate Wilson vibrations of the phenyl ring, where possible).

TABLE 4: Experimental and Calculated Raman Band Positions (cm^{-1}) of Direct Blue 1[a]

experiment[b]						calculated		
KBr	DMSO	water				HF/	B3LYP/	
514.5	530.9	350.6	530.9	647.1	676.4	3-21G	3-21G	description[c]
				1658 w	1658 m	1652 m	1639 w	$\delta(NH_\beta)$ scissor, $\delta(NH_\alpha)$, $\nu(C_9-O_9)$
1620 s	1620 s	1620 vs	1622 s	1622 m			1632 w	$\delta(NH_\beta)$ scissor, $\delta(NH_\alpha)$, $\nu(C_9-O_9)$, δ(naph), ν(N−N)
1597 s		1598 m	1598 vs	1598 vs	1598 vs	1612 vs	1590 vs	ν(Ph) 8a, δ(Ph) 9a, $\delta(NH_\alpha)$
1568 vs	1565 vs	1564 m	1568 vs	1568 m	1567 m	1588 m	1565 m	$\delta(NH_\alpha)$, $\delta(NH_\beta)$ rocking, ν(Ph) 8a, δ(naph), $\nu(C_9-O_9)$
1549 w		1549 m	1547 w	1545 sh	1551 w	1571 w	1537 m	$\delta(NH_\alpha)$, $\delta(NH_\beta)$ scissor, δ(Ph) 18a, δ(Me) rocking, δ(naph), ν(N−N)
1525 s			1525 s	1526 s	1526 s	1542 s	1517 m	ν(Ph) 19a, δ(Ph) 18a, $\nu(C_{11}-N_\rho)$, $\nu(C_{14}-C_{14}')$, δ(Me) umbrella, $\delta(NH_\alpha)$, $\nu(C_9-O_9)$, δ(naph)
1518 sh	1520 m	1519 sh	1517 sh	1518 sh	1518 sh			
1494 sh	1487 w			1490 w	1487 w	1510 m	1478/1496 w	δ(Me) umbrella, $\delta(NH_\alpha)$, δ(Ph)
1455 m		1455 s	1455 m		1457 m	1467 w	1437 m	$\delta(NH_\beta)$ rocking, δ(naph), $\nu(C_9-O_9)$, ν(N−N), δ(Me) umbrella
	1447 w			1449 m				
1421 sh		1420 m	1420 sh	1419 w	1421 w	1434 w	1407 w	$\nu(C_{10}-N_\sigma)$, $\nu(C_7-NH_2)$, $\nu(C_9-O_9)$, δ(naph), $\delta(NH_\beta)$ rocking
1398 s	1392 m		1398 s	1399 s	1401 s	1405 w	1372 w	$\delta(NH_\beta)$ rocking, δ(naph), δ(azo), $\nu(C_{10}-N_\sigma)$
1373 m	1369 m	1373 w	1372 w	1372 m	1376 w	1386 w	1357 w	$\nu(C_{10}-N_\sigma)$, $\delta(NH_\alpha)$, $\nu(C_9-O_9)$, $\delta(NH_\beta)$, $\nu(C_{11}-N_\rho)$, δ(naph)
1324 s	1328 vs		1323 vs	1323 vs	1325 vs	1323 vs	1327 vs	ν(Ph) 14, δ(Ph) 3, $\nu(C_{11}-N_\rho)$, $\nu(C_{14}-C_{14}')$, $\nu(C_{12}-OMe)$, $\delta(NH_\alpha)$, δ(naph)
1310 sh	1307 m	1311 vs	vs	1312 sh	1312 sh	1287 m	1302 w	δ(naph), ν(Ph) 14, δ(Ph) 3, δ(azo), $\delta(NH_\alpha)$, $\delta(NH_\beta)$ rocking
1274 sh			1273 sh				1291 m	ν(Ph) 14, δ(Ph) 9a, $\delta(NH_\alpha)$, δ(azo), δ(Me) umbrella
1255 m	1250 w	1249 w	1249 m		1256 s	1259 m	1269 m	δ(naph), $\delta(NH_\beta)$ rocking, $\nu(C_{11}-N_\rho)$, δ(Ph) 18a
1230 w		1225 w	1231 sh		1235 s			
1193 w	1206 m	1196 s	1193 w		1196 w	1192 w	1242 w	δ(Ph), $\nu(C_{11}-N_\rho)$, $\delta(NH_\alpha)$, $\nu(C_9-O_9)$, δ(naph)
	1185 m							
			1178 sh			1177 w	1207 w	δ(naph), $\delta(NH_\beta)$ rocking, δ(Ph), $\nu(C_{10}-N_\sigma)$, $\nu(C_{12}-OMe)$
1154 m	1153 m	1153 m	1154 m			1157 w	1186 s	ν(N−N), δ(Me), $\nu(C_{12}-OMe)$, $\nu(C_{14}-C_{14}')$, δ(Ph) 9a, δ(naph), $\delta(NH_\alpha)$
1119 m	1117 m	1127 sh	1118 sh			1129 m	1126 m	ν(N−N), ν(Ph) 19a, δ(Ph) 18b, $\delta(NH_\alpha)$
	1090 w							
1053 m						1057 w	1052 w	δ(naph) OOP, $\delta(NH_\beta)$ rocking, $\delta(NH_\alpha)$ OOP
1013 m						1008 w	1014 w	$\delta(NH_\alpha)$ OOP, $\delta(NH_\beta)$ rocking, δ(naph) OOP

[a] Calculated positions are scaled, as outlined in the text. vs = very strong; s = strong; m = medium; w = weak; OOP = out-of-plane mode. [b] Excitation wavelengths in nm. [c] From B3LYP/3-21G calculation, given in decreasing degree of distortion; δ(naph) and δ(Ph) describe a general distortion of a naphthyl or phenyl moiety, respectively (numbers indicate approximate Wilson vibrations of the phenyl ring, where possible).

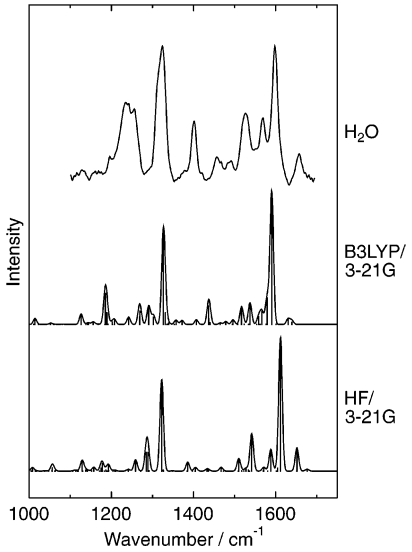

Figure 7. Experimental and calculated Raman spectra of Direct Blue 1. The experimental spectrum was recorded using an excitation wavelength of 676.4 nm; calculated spectra are represented both as discrete lines, scaled to the calculated intensity, and as a calculated spectrum with a fwhm Gaussian bandwidth of 10 cm^{-1} for each vibrational line.

and experimental spectra also gives further confidence in the calculated structure.

An examination of the atomic displacements of the calculated normal modes can be used to consider the nature of the vibrations giving rise to bands in the experimental spectra; all of the B3LYP calculated modes are shown in Supporting Information Figure S3. Tables 3 and 4 give the observed bands in the experimental IR and Raman spectra along with assignments to calculated bands, with descriptions identifying the major contributions to the calculated modes listed in decreasing degree of distortion; the major contributions to each mode were similar for the HF and B3LYP calculations. Figure 8 shows the calculated normal modes assigned here to the two most intense IR and Raman bands: the two IR-active modes are delocalized over most of the molecule, whereas the two Raman-active modes are more localized on the biphenyl moiety. A close examination of the calculated modes reveals several pairs at similar energy which differ only by a phase change about the center of the molecule, resulting in different IR and Raman activities. For example, the normal modes at 1185.3 and 1184.5 cm^{-1} in the B3LYP/3-21G calculation show the largest amount of ν(N−N) character and are shown in Figure 8. The 1185.3-cm^{-1} mode involves both halves of the molecule vibrating in-phase and contributes to the strong calculated Raman band at 1186 cm^{-1}, whereas the 1184.5-cm^{-1} mode involves both halves of the molecule vibrating out-of-phase and contributes to thestrong calculated IR band at 1190 cm^{-1}. The different IR and Raman intensities of these in-phase and out-of-phase combinations arise from the approximately centrosymmetric structure of the dye; they make cross-referencing IR and Raman bands nontrivial, although many of these pairs of modes do not contribute strongly to the spectra.

Generally, the normal modes are very mixed, with contributions from displacements within several parts of the molecule. For example, nearly every calculated normal mode in the range 1000−1650 cm^{-1} involves a contribution from an N−H bending motion. Consequently, the notion of assigning individual bands to particular group frequencies is not always helpful. Nonetheless, calculated normal modes near 1650 cm^{-1} which contain a large component of ν(C═O) occur within the group frequency

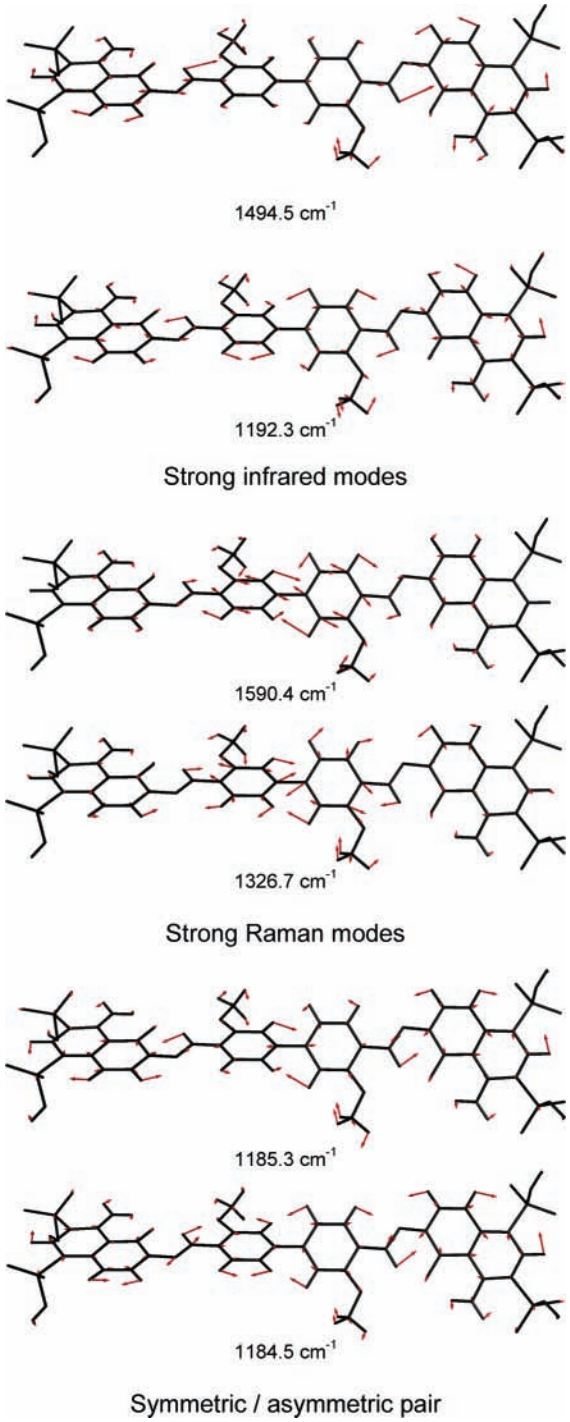

Figure 8. Atomic displacements for selected vibrational modes of Direct Blue 1 calculated at the B3LYP/3-21G level: those giving the two most intense bands in the IR and Raman spectra, respectively, and an example of symmetric and asymmetric modes with similar energies.

range of ca. 1600−1850 cm^{-1} for carbonyl groups[63,64] and much higher than the ν(C−O) band at 1224 cm^{-1} in phenol,[64] consistent with the hydrazone structure. Where possible, standard Wilson notation[65] has been used in Tables 3 and 4 to label vibrations involving the phenyl rings.

There have been relatively few full assignments[18,19,66] and vibrational calculations[15−17,20,21,67] of azo dyes and similar compounds. Nevertheless, the assignments determined from ab initio calculations on Direct Blue 1 compare relatively well with previous reports on similar dyes, although it is difficult to make direct comparisons because of the highly coupled nature of the vibrations. The large amount of mixing in the normal modes of

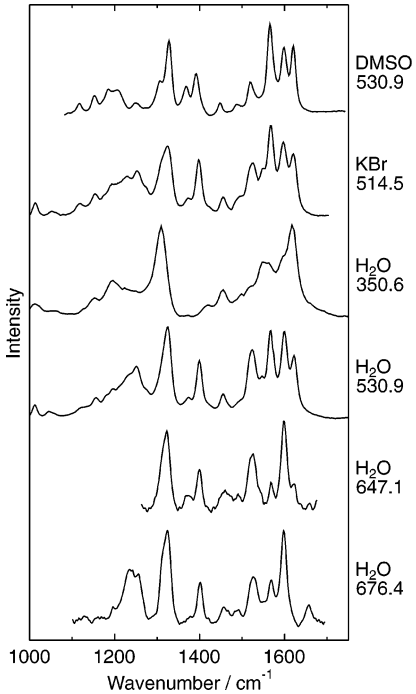

Figure 9. Experimental resonance Raman spectra of Direct Blue 1 in DMSO, KBr, and water recorded with a range of excitation wavelengths (in nm).

Direct Blue 1 may be due to the approximately symmetrical structure of this dye; for example, stretching of the N−N bond in Direct Blue 1 occurs simultaneously in both halves of the molecule, causing significant distortion in the central biphenyl moiety. For a simple mono-azo dye, this distortion of other moieties may be much less pronounced, as reported for Solvent Yellow 14,[17] where the normal mode displacements appear to be localized predominantly on either the naphthyl ring, the phenyl ring, or the hydrazone group; however, it was noted that there is no single N−N stretching mode for Solvent Yellow 14, with several modes involving a significant displacement of the hydrazone group.

Some direct comparisons can be drawn between assignments for azo dyes in the literature and the assignments presented here for Direct Blue 1. The calculated Raman band at ca. 1185 cm^{-1}, discussed already, which contains the largest ν(N−N) contribution, is consistent with the reported positions of the ν(N−N) bands of other hydrazone dyes (e.g. the experimental bands at 1230 cm^{-1} for Orange II[19] and at 1150 cm^{-1} for Solvent Yellow 14[17]); by contrast, the ν(N═N) band is observed at ca. 1440 cm^{-1} for azobenzene dyes.[20,21] The experimental Raman band of Direct Blue 1 at 1376 cm^{-1}, which is assigned to a normal mode containing a large $\nu(C_{10}-N_{\alpha})$ contribution, compares well with the experimental Raman band at 1389 cm^{-1} for Orange II which was assigned to a ν(C−N) vibration.[66] Other experimental Raman bands of Direct Blue 1 at 1598 and 1487 cm^{-1}, which are assigned to modes involving large distortions of the central biphenyl moiety, are comparable to experimental bands at 1598 cm^{-1} for Solvent Yellow 14[17] and 1482 cm^{-1} for the phenylazonaphthol pigment Ca4B,[18] both of which are assigned to phenyl ring modes.

Resonance Raman Spectroscopy. To gain further insights into the electronic structure of Direct Blue 1, resonance Raman spectra at several excitation wavelengths were recorded from aqueous samples, as shown in Figure 9 along with resonance Raman spectra of Direct Blue 1 in DMSO solution and KBr. The Raman spectra show complex changes in relative band intensities as the excitation wavelength is brought into resonance with the visible and UV absorption bands; absolute intensities were not determined, but relative intensities may be compared within spectra recorded at different excitation wavelengths.

The relative intensities of the strongest bands observed in the off-resonance Raman spectrum (λ_{ex} = 676.4 nm), at 1598, 1526, 1401, and 1325 cm^{-1}, remain fairly constant as the excitation wavelength is changed to 647.1 and 530.9 nm; several other bands, such as those at 1622 and 1568 cm^{-1}, show an increase in relative intensity, and those at 1658 and 1487 cm^{-1} show a decrease in relative intensity. The relative enhancement of these bands may be considered in terms of the changes in electron density indicated by the excited-state calculations (Figure 4, Table 2). The lowest-energy electronic transition was calculated to involve electron transfer from the biphenyl group onto the carbonyl groups and one of the hydrazone nitrogens, as well as charge redistribution within the naphthyl rings. This transition would be expected to cause some distortion within most of the molecule, giving some resonance enhancement to many of the Raman bands. The observed Raman bands do show differing amounts of relative enhancement as the excitation wavelength is brought into resonance with the visible absorption band, but there are no bands which become dominant. The disappearance of the band at 1658 cm^{-1} on tuning into resonance with the visible absorption band suggests that this vibrational mode is not coupled to the electronic transition. This band is assigned to a mode with scissor distortion of the NH_2 groups as the major component (Table 4), consistent with the calculated resonant electronic transition which does not involve a change in the electron density at the NH_2 groups (Figure 4). The band at 1620 cm^{-1} also involves a large scissor distortion of the NH_2 groups, but δ(naph) and ν(N−N) distortions contribute also and can account for its gain in relative intensity in resonance with this transition.

UV excitation (λ_{ex} = 350.6 nm) results in a large increase in intensity of the band at 1311 cm^{-1} relative to that at 1325 cm^{-1}, and the band at 1620 cm^{-1} is also enhanced relative to other bands. The Raman bands at 1311 and 1325 cm^{-1} are assigned to modes which are predominantly naphthyl- and phenyl-based, respectively, and the enhancement of the 1311 cm^{-1} band relative to the 1325 cm^{-1} band suggests that UV excitation at 350.6 nm is resonant with a naphthyl-based electronic transition. The excited-state calculations gave several weak electronic transitions in the near-UV region which can be described as being predominantly naphthyl-based transitions (Figure 4, Table 2, and Supporting Information). Excitation in resonance with this type of electronic transition would be expected to give enhancement of bands associated with vibrations of the naphthyl and NH_2 groups relative to those of the biphenyl moiety, as observed here experimentally.

NMR Spectroscopy. The B3LYP/mixed basis set optimized structure of Direct Blue 1 was used to calculate ^1H and ^{13}C NMR resonances for Direct Blue 1 using the B3LYP method with both the mixed basis set and the standard 6-31G(d) basis set, using the GIAO algorithm. Each half of the molecule gives NMR resonances which are generally within <1% of the equivalent resonance in the other half of the molecule. Calculated NMR resonances averaged from both sides of the molecule, and relative to tetramethylsilane (TMS) resonances calculated at the same level of theory, are given in Table 5 along with experimental values for Direct Blue 1 in DMSO-d_6 which have been assigned using experimental 2D-NMR data.[35]

In general, the calculated NMR values compare well with the experimental values, with the majority being within 5%. The H_{α}, $H_{\beta 1}$, and $H_{\beta 2}$ resonances are calculated well, being

TABLE 5: Experimental and Calculated ^{1}H and ^{13}C NMR Shifts (ppm) and Assignments for Direct Blue 1

	experiment[a]		calculated[b]			
	DMSO-d_6		B3LYP/mixed basis set[c]		B3LYP/6-31G(d)	
atom	H	C	H	C	H	C
1	7.02	127.9	7.37	131.0	7.12	129.9
2	7.99	121.9	7.96	112.9	7.65	113.7
3		135.7		136.6		137.6
4		121.8		118.0		117.7
5	8.37	132.8	8.61	133.2	8.21	133.7
6		127.1		111.0		110.4
7		150.3		147.4		146.2
8		113.7		112.9		111.8
9		181.3		171.8		173.5
10		133.6		129.4		128.7
11		130.4		126.5		125.7
12		148.6		145.3		144.0
13	7.51	110.1	6.72	105.1	6.67	104.6
14		137.4		135.9		135.5
15	7.52	120.4	7.02	115.6	7.08	115.5
16	7.89	115.3	8.18	112.1	7.89	111.9
17	4.14	56.8	4.26	54.2	4.00	55.3
α	15.77		15.58		14.76	
β1	7.5		7.80		6.88	
β2	9.7		11.01		10.05	

[a] Reference 35. [b] Averages from equivalent atoms in each half of the molecule. [c] Basis set: 6-31+G(d) for N, S, and O; 6-31G(d) for C; and 3-21G for H.

further upfield than the aromatic proton resonances as a result of the hydrogen bonding to adjacent oxygen atoms; the aromatic protons give a qualitative match with the experimental resonances but are calculated less well, with some being upfield and others being downfield from the experimental resonances. The calculated ^{13}C resonances match the experimental values reasonably well and would greatly assist the assignment of experimental spectra in the absence of any 2D-NMR data, because the molecule contains many aromatic carbon atoms. Our studies of Direct Blue 1 in solution show that the ^{1}H NMR spectrum is affected more strongly by solvent than the ^{13}C NMR spectrum;[35] a similar difference between calculated and experimental ^{1}H NMR positions has also been reported for 4,6-dimethyl-2-mercaptopyrimidine,[68] where large errors in certain calculated ^{1}H resonances were attributed to solvation effects acting on specific protons. The 6-31G(d) basis set did not give any significant improvement over the mixed basis set, with some positions being calculated closer to the experimental values and others calculated further away (Table 5). The literature recommends the use of significantly larger basis sets for the calculation of NMR shifts,[69,70] but our attempts to do so for Direct Blue 1 were unsuccessful; nevertheless, our calculations show that the complicated experimental NMR spectrum of this large molecule can be assigned with the assistance of calculations using a relatively small basis set.

Conclusions and Applicability of Methods

The bis-azo dye Direct Blue 1 has been the subject of a detailed computational study using a range of semiempirical and ab initio methods to calculate a range of structural and spectroscopic properties. The results from these calculations have been compared with experimental results for Direct Blue 1 and similar compounds, and it has been shown that the comparison is good, for both structure and spectroscopy. The ground-state structure is modeled well by the AM1 semiempirical method as well as by the more computationally demanding ab initio methods. Both the semiempirical ZINDO method and ab initio TD-DFT methods have provided an insight into the electronic structure and transitions of this large bis-azo dye. The vibrational spectra are modeled poorly by the AM1 method, instead requiring ab initio methods which reproduce the spectra well using a smaller basis set than would routinely be used for vibrational calculations of smaller molecules. The observed resonance enhancement trends in the experimental Raman spectra are consistent with the calculated excited states. The NMR resonances of Direct Blue 1 are calculated adequately using a DFT method, and such calculations would be extremely useful in assigning experimental spectra of similar dyes.

These studies demonstrate that useful insights into molecular structure and spectroscopy can be gained for a relatively large molecule using an appropriate level of theory, and they complement a very recent computational and experimental study of bis-azo pigments.[71] The results presented here show that a wide range of calculations can assist with analyzing the structure and spectroscopy of large dyes, and such computational studies need not be restricted to studies of small model compounds.

Acknowledgment. We acknowledge Reuben Girling for assistance with recording Raman spectra and Heather Fish for recording the NMR spectra. We acknowledge the support of Unilever Research.

Supporting Information Available: Additional details of calculated excited states, and calculated displacement vectors and IR and Raman intensities for all 258 normal modes. This information is available free of charge via the Internet at http://pubs.acs.org.

References and Notes

(1) Zollinger, H. *Color Chemistry*, 3rd ed.; Wiley-VCH: Weinheim, 2003.
(2) Ojala, W. H.; Ojala C. R.; Gleason, W. B. *Antiviral Chem. Chemother.* **1995**, *6*, 25.
(3) Ojala, W. H.; Sudbeck, E. A.; Lu, L. K.; Richardson, T. I.; Lovrien, R. E.; Gleason, W. B. *J. Am. Chem. Soc.* **1996**, *118*, 2131.
(4) Tsopelas, C.; Sutton, R. *J. Nucl. Med.* **2002**, *43*, 1377.
(5) Rasmussen, P. H.; Ramanujam, P. S.; Hvilsted, S.; Berg, R. H. *J. Am. Chem. Soc.* **1999**, *121*, 4738.
(6) Åstrand, P.-O.; Ramanujam, P. S.; Hvilsted, S.; Bak, K. L.; Sauer, S. P. A. *J. Am. Chem. Soc.* **2000**, *122*, 3482.
(7) Kawata, S.; Kawata, Y. *Chem. Rev.* **2000**, *100*, 1777.
(8) Olivieri, A. C.; Wilson, R. B.; Paul, I. C.; Curtin, D. Y. *J. Am. Chem. Soc.* **1989**, *111*, 5525.
(9) Kennedy, A. R.; McNair, C.; Smith, W. E.; Chisholm, G.; Teat, S. J. *Angew. Chem., Int. Ed.* **2000**, *39*, 638.
(10) Ojala, W. H.; Lu, L. K.; Albers, K. E.; Gleason, W. B. *Acta Crystallogr., Sect. B* **1994**, *50*, 684.
(11) Malone, J. F.; Andrews, S. J.; Bullock, J. F.; Docherty, R. *Dyes Pigm.* **1996**, *30*, 183.
(12) Kennedy, A. R.; Hughes, M. P.; Monaghan, M. L.; Staunton, E.; Teat, S. J.; Smith, W. E. *J. Chem. Soc., Dalton Trans.* **2001**, 2199.
(13) Park, K.-M.; Yoon, I.; Lee, S. S.; Choi, G.; Lee, J. S. *Dyes Pigm.* **2002**, *54*, 155.
(14) Anderson, S.; Clegg, W.; Anderson, H. L. *Chem. Commun.* **1998**, 2379.
(15) Bell, S.; Bisset, A.; Dines, T. *J. Raman Spectrosc.* **1998**, *29*, 447.
(16) Pajak, J.; Ramaekers, R.; Rospenk, M.; Alexandrov, V.; Stepanian, S.; Adamowicz, L.; Maes, G. *Chem. Phys.* **2003**, *286*, 193.
(17) Munro, C. H.; Smith, E. W.; Armstrong, D. R.; White, P. C. *J. Phys. Chem.* **1995**, *99*, 879.
(18) Clarkson, J.; Armstrong, D. R.; Munro, C. H.; Smith, W. E. *J. Raman Spectrosc.* **1998**, *29*, 421.
(19) Bauer, C.; Jacques, P.; Kalt, A. *Chem. Phys. Lett.* **1999**, *307*, 397.
(20) Biswas, N.; Umapathy, U. *J. Phys. Chem. A* **2000**, *104*, 2734.
(21) Armstrong, D. R.; Clarkson, J.; Smith, W. E. *J. Phys. Chem.* **1995**, *99*, 17825.
(22) Tackley, D. R.; Dent, G.; Smith, W. E. *Phys. Chem. Chem. Phys.* **2000**, *2*, 3949.
(23) Tackley, D. R.; Dent, G.; Smith, W. E. *Phys. Chem. Chem. Phys.* **2001**, *3*, 1419.

(24) Nepraš, M.; Lunák, S., Jr.; Hrhdina, R. *Chem. Phys. Lett.* **1989**, *159*, 366.
(25) Fabian, J.; Diaz, L. A.; Seifert, G.; Niehaus, T. J. *THEOCHEM* **2002**, *594*, 41.
(26) Cattaneo, P.; Persico, M. *Phys. Chem. Chem. Phys.* **1999**, *1*, 4739.
(27) Morley, J. O.; Charlton, M. H. *J. Phys. Chem.* **1995**, *99*, 1928.
(28) Stoyanov, St.; Iijima, T.; Stoyanova, T.; Antonov, L. *Dyes Pigm.* **1995**, *27*, 237.
(29) Rau, H. *Angew. Chem., Int. Ed. Eng.* **1973**, *12*, 224.
(30) (a) Dewar, M. J. S.; Thiel, W. *J. Am. Chem. Soc.* **1977**, *99*, 4899. (b) Dewar, M. J. S.; McKee, M. L.; Rzepa, H. S. *J. Am. Chem. Soc.* **1978**, *100*, 3607. (c) Dewar, M. J. S.; McKee, M. L. *J. Comput. Chem.* **1983**, *4*, 84. (d) Dewar, M. J. S.; Reynolds, C. H. *J. Comput. Chem.* **1986**, *7*, 140.
(31) (a) Stewart, J. J. P. *J. Comput. Chem.* **1989**, *10*, 209. (b) Stewart, J. J. P. *J. Comput. Chem.* **1989**, *10*, 221.
(32) (a) Dewar, M. J. S.; McKee, M. L.; Rzepa, H. S. *J. Am. Chem. Soc.* **1978**, *100*, 3607. (b) Dewar, M. J. S.; Zoebisch, E. G.; Healy, E. F.; Stewart, J. J. P. *J. Am. Chem. Soc.* **1985**, *107*, 3902. (c) Dewar, M. J. S.; Reynolds, C. H. *J. Comput. Chem.* **1986**, *7*, 140.
(33) Young, D. C. *Computational Chemistry*; John Wiley & Sons: Toronto, 2001.
(34) Abbott, L. C.; MacFaul, P.; Jansen, L.; Oakes, J.; Lindsay Smith, J. R.; Moore, J. N. *Dyes Pigm.* **2001**, *48*, 49.
(35) Abbott, L. C.; Batchelor, S. N.; Jansen, L.; Oakes, J.; Lindsay Smith, J. R.; Moore, J. N. *New J. Chem.* **2004**, *28*, 815.
(36) Abbott, L. C.; Batchelor, S. N.; Oakes, J.; Lindsay Smith, J. R.; Moore, J. N. *J. Phys. Chem. B.* **2004**, *108*, 13726.
(37) Robinson, C.; Mills, H. A. T. *Proc. R. Soc. London, Ser. A* **1931**, *131*, 576.
(38) Frisch, M. J.; Trucks, G. W.; Schlegel, H. B.; Scuseria, G. E.; Robb, M. A.; Cheeseman, J. R.; Zakrzewski, V. G.; Montgomery, J. A., Jr.; Stratmann, R. E.; Burant, J. C.; Dapprich, S.; Millam, J. M.; Daniels, A. D.; Kudin, K. N.; Strain, M. C.; Farkas, O.; Tomasi, J.; Barone, V.; Cossi, M.; Cammi, R.; Mennucci, B.; Pomelli, C.; Adamo, C.; Clifford, S.; Ochterski, J.; Petersson, G. A.; Ayala, P. Y.; Cui, Q.; Morokuma, K.; Malick, D. K.; Rabuck, A. D.; Raghavachari, K.; Foresman, J. B.; Cioslowski, J.; Ortiz, J. V.; Stefanov, B. B.; Liu, G.; Liashenko, A.; Piskorz, P.; Komaromi, I.; Gomperts, R.; Martin, R. L.; Fox, D. J.; Keith, T.; Al-Laham, M. A.; Peng, C. Y.; Nanayakkara, A.; Gonzalez, C.; Challacombe, M.; Gill, P. M. W.; Johnson, B. G.; Chen, W.; Wong, M. W.; Andres, J. L.; Head-Gordon, M.; Replogle, E. S.; Pople, J. A. *Gaussian 98*, revision A.7; Gaussian, Inc.: Pittsburgh, PA, 1998.
(39) Mayo, S. L.; Olafson, B. D.; Goddard, W. A. *J. Phys. Chem.* **1990**, *94*, 8897.
(40) (a) Becke, A. D. *J. Chem. Phys.* **1993**, *98*, 5648. (b) Lee, C.; Yang, W.; Parr, R. G. *Phys. Rev. B* **1988**, *37*, 785.
(41) (a) Anderson, W. P.; Edwards, W. D.; Zerner, M. C. *Inorg. Chem.* **1986**, *25*, 2728. (b) Ridley, J.; Zerner, M. C. *Theor. Chim. Acta* **1973**, *32*, 111. (c) Edwards, W. D.; Ohrn, N. Y.; Weiner, B. L.; Zerner, M. C. *Int. J. Quantum Chem., Quantum Chem. Symp.* **1984**, *18*, 507.
(42) Casida, M. E.; Jamorski, C.; Casida, K. C.; Salahub, D. R. *J. Chem. Phys.* **1998**, *108*, 4439.
(43) Wolinski, K.; Hilton, J. F.; Pulay, P. *J. Am. Chem. Soc.* **1990**, *112*, 8251.
(44) Portman, S.; Lüthi, H. P. *Chimia* **2000**, *54*, 766. *Molekel*, www.cscs.ch/molekel/.
(45) Schaftenaar, G.; Noordik, J. H. *J. Comput.-Aided Mol. Des.* **2000**, *14*, 123.
(46) A starting geometry with the two halves of the molecule in a syn conformation around the central biphenyl bond gave an AM1 optimized geometry that was ca. 0.6 kJ mol^{-1} higher in energy than the respective anti conformer. A starting geometry with the methoxy groups in an anti conformation with respect to the hydrazone NH groups gave an AM1 optimized geometry that was twisted significantly from planarity about the biphenyl−N bonds, and it was ca. 22.3 kJ mol^{-1} higher in energy than that of the respective syn conformer; furthermore, a close examination of our previously reported experimental NMR data[35] shows a NOESY interaction between H_1 and H_{16} (see Figure 2), providing additional support for the presence of this syn conformer.
(47) Skowronek, M.; Roterman, I.; Konieczny, L.; Stopa, B.; Rybarska, J.; Piekarska, B.; Górecki, A.; Król, M. *Comput. Chem.* **2000**, *24*, 429.
(48) Almeningen, A.; Bastiansen, O.; Fernholt, L.; Cyvin, B. N.; Cyvin, S. *J. Mol. Struct.* **1986**, *128*, 59.
(49) Tsuzuki, S.; Tanabe, K. *J. Phys. Chem.* **1991**, *95*, 139.
(50) Lee, S. Y. *Bull. Korean Chem. Soc.* **1998**, *19*, 93.
(51) Göller, A.; Grummt, U.-W. *Chem. Phys. Lett.* **2000**, *321*, 399.
(52) Robertson, G. B. *Nature* **1961**, *191*, 593.
(53) Trotter, J. *Acta Crystallogr.* **1961**, *14*, 1135.
(54) Gilli, P.; Bertolasi, V.; Pretto, L.; Lyčka, A.; Gilli, G. *J. Am. Chem. Soc.* **2002**, *124*, 13554.
(55) *Tables of Interatomic Distances and Configuration in Molecules and Ions*; Mitchell, A. D., Cross, L. C., Eds.; The Chemical Society: London, 1958.
(56) Dos Santos, H. F.; De Oliveira, L. F. C.; Dantas, S. O.; Santos, P. S.; De Almeida, W. B. *Int. J. Quantum Chem.* **2000**, *80*, 1076.
(57) (a) Perdew, J. P.; Burke, K.; Ernzerhof, M. *Phys. Rev. Lett.* **1996**, *77*, 3865. (b) Adamo, C.; Barone, V. *J. Chem. Phys.* **1999**, *110*, 6158. (c) Adamo, C.; Scuseria, G. E.; Barone, V. *J. Chem. Phys.* **1999**, *111*, 2889.
(58) Guillaumont, D.; Nakamura, S. *Dyes Pigm.* **2000**, *46*, 85.
(59) Linear fits of calculated to experimental wavenumbers with a variable offset ($y = mx + c$) for AM1, HF/3-21G, and B3LYP/3-21G calculations gave $m = 1.2749$, 1.2040, and 0.9983, and $c = -184$, −140, and 32, with R^2 values of 0.978, 0.985, and 0.994, respectively; the simple linear fits ($y = mx$) gave values of $m = 1.1479$, 1.1051, and 1.0213, with R^2 values of 0.968, 0.979, and 0.993 (Figure 5), respectively, and provided the scaling factors used here.
(60) Scott, A. P.; Radom, L. *J. Phys. Chem.* **1996**, *100*, 16502.
(61) Halls, M. D.; Schlegel, H. B. *J. Chem. Phys.* **1998**, *109*, 10587.
(62) Halls, M. D.; Schlegel, H. B. *J. Chem. Phys.* **1999**, *111*, 8819.
(63) Dollish, F. R.; Fateley, W. G.; Bentley, F. F. *Characteristic Raman Frequencies of Organic Compounds*; John Wiley and Sons: New York, 1974.
(64) Silverstein, R. M.; Webster, F. X. *Spectrometric Identification of Organic Compounds*, 6th ed.; John Wiley and Sons: New York, 1998.
(65) Wilson, E. B. *Phys. Rev.* **1934**, *45*, 706.
(66) Barnes, A. J.; Majid, M. A.; Stuckey, M. A.; Gregory, P.; Stead, C. V. *Spectrochim. Acta, Part A* **1985**, *41*, 629.
(67) Fliegl, H.; Köhn, A.; Hättig, C.; Ahlrichs, R. *J. Am. Chem. Soc.* **2003**, *125*, 9821.
(68) Martos-Calvente, R.; de la Peña O'Shea, V. A.; Campos-Martin, J. M.; Fierro, J. L. G. *J. Phys. Chem. A* **2003**, *107*, 7490.
(69) Bagno, A. *Chem.—Eur. J.* **2001**, *7*, 1652.
(70) Cheeseman, J. R.; Trucks, G. W.; Keith, T. A.; Frisch, M. J. *J. Chem. Phys.* **1996**, *104*, 5497.
(71) Dines, T. J.; Onoh, H. *J. Raman Spectrosc.* **2004**, *35*, 284.